

Electron-correlation effects in double-electron-capture collisions of 60-keV C^{6+} with He

N. Stolterfoht* and K. Sommer

Hahn-Meitner-Institut Berlin GmbH, D-1000 Berlin 39, Federal Republic of Germany

J. K. Swenson,[†] C. C. Havener, and F. W. Meyer

Oak Ridge National Laboratory, Physics, Division, Oak Ridge, Tennessee 37831

(Received 13 February 1990; revised manuscript received 21 May 1990)

The method of zero-degree Auger spectroscopy was used to measure cross sections for the production of K and L Auger electrons by double electron capture in 60-keV $C^{6+} + He$ collisions. Corresponding atomic-structure calculations were performed to determine the related Auger and x-ray transition rates. The resulting Auger yields are found to deviate significantly from unity. The Auger yields were applied to evaluate cross sections for the production of the configuration $3lnl'$ ($n = 3$ to 5) and $2lnl'$ ($n = 3$ to 8). These data are found to compare well with experimental results obtained previously for the isocharged system $O^{6+} + He$. Comparison is also made with recent calculations including the electron-electron interaction. It is shown that electron-correlation effects play a significant role for double electron capture in the studied collision system.

I. INTRODUCTION

In the past few years, the study of double electron capture by highly charged projectiles incident on few-electron target atoms at low collision energies has received a great deal of attention. By measuring total double-capture cross sections for the collision system 40-keV $C^{4+} + He$, Crandall *et al.*¹ were the first to show that double capture is an important process in slow, multicharged ion-atom collisions. For this system two-electron transfer had been interpreted in terms of a one-step process where the electron-electron interaction plays an important role.^{2,3} More recently, state-selective double capture has been studied by the methods of translational spectroscopy⁴⁻⁶ and electron spectroscopy.⁷⁻¹² These more recent experiments have been interpreted either in terms of the one-step process produced by electron-correlation effects^{8,10,13} or in terms of two successive single-electron transitions^{14,15} caused by nucleus-electron interaction. These latter transitions may also occur simultaneously when the associated transition regions overlap as shown by Barat and collaborators.¹⁶ In accordance with related work,^{17,18} the process involving uncorrelated transitions produced by the nucleus-electron interaction will be referred to as a two-step process.

In a series of papers^{8,19-23} we reported on measurements of double capture in 60-keV $O^{6+} + He$ collisions. In that work we proposed a direct method of verifying effects of electron correlation in double electron capture in slow, multicharged ion-atom collisions. The correlated-double-capture (CDC) process produces the nonequivalent electron configurations $2pnl$ ($n \geq 6$), while the uncorrelated double capture creates the configurations $3l3l'$ (or $2l3l'$) of equivalent (or nearly equivalent) electrons. These electrons are added to the oxygen $1s^2$ core which is not explicitly indicated here. It is noted that the production of the equivalent electron

configuration $3l3l'$ may also involve correlation effects.⁸ The important point of this method is that the states involving equivalent and nonequivalent electrons decay by Coster-Kronig and L Auger transitions, respectively, and that they can readily be distinguished using high-resolution electron spectroscopy. Recent improved experiments²⁰ for the system 60-keV $O^{6+} + He$ yield a fraction of 0.3 for the production cross section of the $2pnl$ configuration with $n \geq 6$ relative to the summed cross sections for the production of the configurations $2pnl$ ($n \geq 6$) and $3lnl'$ ($n \geq 3$). From this finding we concluded that double capture in 60-keV $O^{6+} + He$ collisions involves significant electron-correlation effects.^{8,20} Similar conclusions have been drawn by Mann and Schulte¹⁰ and Tanis *et al.*²⁴

The observation of the Coster-Kronig electrons in $O^{6+} + He$ collisions created an interesting discussion about the relevance of electron-correlation effects in slow, multicharged ion-atom collisions. From energy-loss measurements, Barat and collaborators¹⁶ concluded that correlation effects are negligible in double electron capture for $O^{8+} + He$ collisions, but this conclusion could not be substantiated for the $O^{6+} + He$ system. Recently, Roncin *et al.*²⁵ confirmed that correlation effects are important in $O^{6+} + He$ collisions. From measurements at relatively low energies of 9 keV, Roncin *et al.*²⁵ concluded that single capture into the $3d$ orbital of oxygen followed by a correlated transfer excitation (CTE) process is dominant. This CTE process has been previously suggested by Winter *et al.*²⁶ and has been considered also in our work.^{19,23,27} However, at higher impact energies we would expect²³ that the CDC process proposed previously in our work^{8,19} gains importance relative to the CTE process. As a result of this apparent lack of consensus, we feel that further work is needed to analyze the different mechanisms involved in double capture at energies as high as 60 keV.

Aside from the discussion of electron correlation effects, the Coster-Kronig electrons produced in 60-keV $O^{6+} + He$ collisions have also become a matter of controversy because of the lack of agreement of the relative intensity of these electrons measured by different groups. Mack and Niehaus⁹ and Bordenave-Montesquieu *et al.*²⁸ found relative Coster-Kronig line intensities which are much smaller (by a factor of about 4) than our results,²⁰ whereas measurements by Mann and Schulte¹⁰ and Chantrenne *et al.*¹¹ supported our results. It had initially been suggested that possible alignment effects might produce the observed discrepancies,²⁷ but this supposition was found to be invalid.²⁰ Therefore other reasons for the observed discrepancies need to be considered. In the $O^{6+} + He$ system the decay of states associated with the $2pnl$ configuration gives rise to electrons which have relatively low energies near 10 eV. At these low energies it is difficult to avoid instrumental effects influencing the collection efficiency of the electron analyzer. Hence, to obtain conclusive results about the production of the $2pnl$ configurations it would be desirable to employ a method other than the detection of the Coster-Kronig electrons.

Such method exists for the collision system $C^{6+} + He$. Since the systems $C^{6+} + He$ and $O^{6+} + He$ are isocharged, it can be expected that the dynamics of the double-capture process are similar for both systems. The essential difference between the two systems is the missing 1s electrons in C^{6+} which strongly reduces the quantum defect. This results in a negligible energy splitting between the 2s and 2p subshells. The Coster-Kronig transitions are thus not possible for the Rydberg electron of interest here. Rather, the states due to the $2lnl'$ configurations decay by *K*-shell Auger transitions which produce electrons of several hundred eV. The much higher energies of the *K* Auger electrons can be measured without the instrumental problems generally involved in the detection of the Coster-Kronig electrons. In addition, the occupation of both the 2s and 2p subshells as well as Rydberg levels *n* as small as 3 can be observed.

In this work we measured the double capture in 60-keV $C^{6+} + He$ collisions. We calculated also x-ray and Auger transition rates by means of a Hartree-Fock atomic-structure code²⁹ which indicates a significant deviation of the related Auger yield from 1. Using the theoretical Auger yield we determined cross sections for the production of the configurations $2l6l'$ and $2l7l'$ which are consistent with our previous results for the $O^{6+} + He$ system. In addition, we obtain cross section results for the configurations $2l3l'$, $2l4l'$, and $2l5l'$ which could not be observed for the $O^{6+} + He$ system. The production of these configurations will be discussed from the perspective of electron-correlation effects occurring during the collision. It is noted that preliminary results of our measurements have been presented recently.³⁰

II. EXPERIMENTAL METHOD AND RESULTS

The principle of our method is illustrated in Fig. 1, which shows the orbital electron energies of the $(C+He)^{6+}$ system. In the incident channel two electrons occupy the He 1s orbital which crosses the 3*l* orbital of

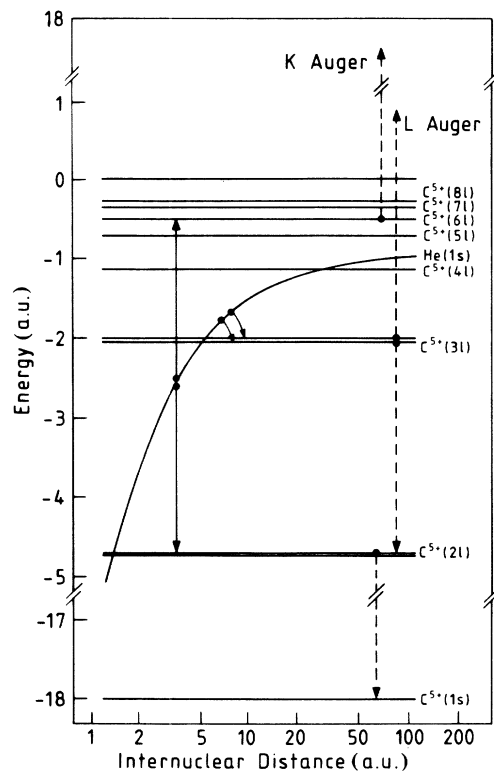


FIG. 1. Diagram of the orbital electron energies for the system $(C+He)^{6+}$ showing correlated and uncorrelated two-electron captures. These processes produce configurations decaying by *K* Auger and *L* Auger electron emission, respectively.

carbon near 5 a.u. In this region the uncorrelated double electron capture may occur by two independent one-electron transitions creating the configurations $3l3l'$ (or $2l3l'$) of equivalent (or near equivalent) electrons. It is noted that due to orbital relaxation the second transition into the 3*l* shell may occur at distances larger than 5 a.u. As the internuclear distance continues to decrease, resonance conditions are created for the CDC process in which one electron is transferred into the 2*p* orbital while another electron is excited into a Rydberg level *nl*. Alternatively, the 2*p* and *nl* orbitals may be populated by one-electron capture into the 3*l* orbital followed by a CTE process.²⁶ The doubly excited states associated with the configurations $2lnl'$ and $3lnl'$ autoionize giving rise to *K* Auger and *L* Auger electrons, respectively. Thus the production of nonequivalent and equivalent electron configuration can be studied by means of high-resolution Auger spectroscopy.

Since the experimental method has been described before,^{8,20} only a brief outline is given here. The measurements were carried out at the electron cyclotron resonance (ECR) source at Oak Ridge National Laboratory using the electron-spectroscopy apparatus temporarily transported from the Hahn-Meitner-Institut Berlin. Electron spectra produced by 60-keV $C^{6+} + He$ collisions were measured by means of the 0° Auger spectroscopy method extensively applied in the past.^{31,32} A C^{6+} beam

was extracted from the ECR source and collimated to a diameter of 2 mm. Typical beam currents of about 1 nA were collected in a Faraday cup and were used to normalize the spectra. In the scattering chamber the beam passed through a gas cell of 5 cm length within which a pressure of about 10^{-4} Torr of He was maintained. During operation of the cell the pressure in the scattering chamber was $\sim 10^{-6}$ Torr. We observed a certain line intensity due to Li-like configurations (e.g., $1s2s2p$) which can only be produced by multiple collisions. For the production cross sections of the configurations $2lnl'$ and $3lnl'$ and the corresponding Auger peak structures no pressure dependencies were found. Hence we assume that charge changing collisions may occur in the beam line or at slit edges producing C^{5+} before entering the scattering chamber.

Electrons produced in the target cell were observed at an angle of 0° with respect to the incident beam direction using a tandem electron spectrometer consisting of two consecutive 90° parallel-plate analyzers. The entrance analyzer was used to deflect the electrons out of the ion beam as well as to suppress background electrons. The exit analyzer determined the electron energy with high resolution. The intrinsic resolution of the exit analyzer was 7.5% [full width at half maximum (FWHM)]. A constant energy resolution of 1.5 eV was achieved by deceleration of the electrons in the region between the two analyzers to 20 eV. The electron acceptance angle was 1° (FWHM), which was small enough to avoid kinematic line-broadening effects.

Typical examples of the measured K and L Auger electron spectra are shown in Figs. 2 and 3, respectively. Figure 2 indicates the peak structure associated with the configurations $2lnl'$ ($n \geq 3$), whereas Fig. 3 shows the spectra attributed to the configurations $3lnl'$ ($n = 3$ to 6). It should be noted that K Auger lines associated with the

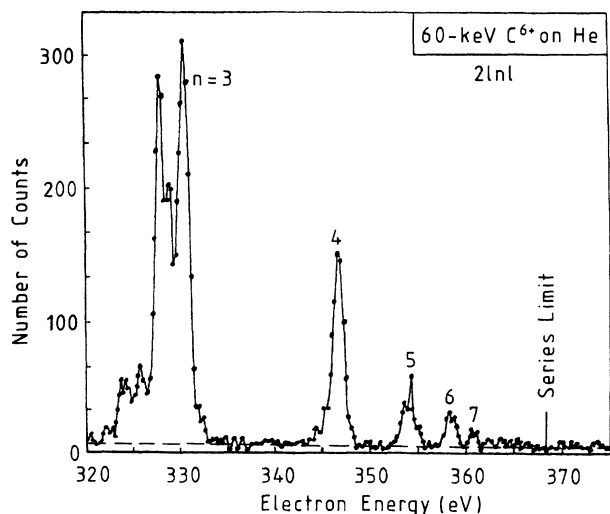


FIG. 2. Spectrum of K Auger electrons produced in 60-keV $C^{6+} + He$ collisions. Each peak corresponds to the decay of states associated with a configuration $2lnl'$ where $n = 3$ to 7.

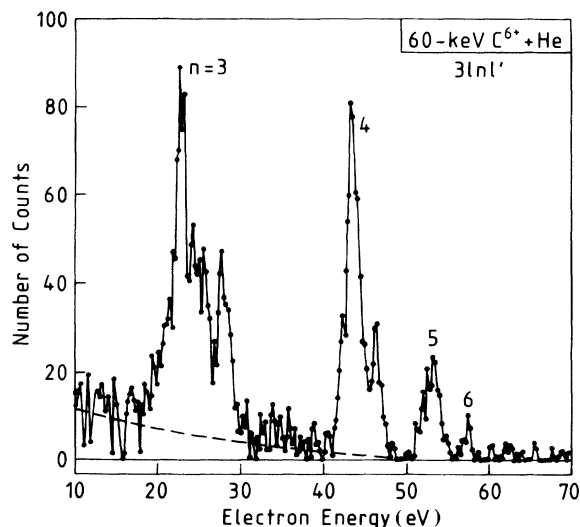


FIG. 3. Spectrum of L Auger electrons produced in 60-keV $C^{6+} + He$ collisions. Each peak corresponds to the decay of states associated with a configuration $3lnl'$ where $n = 3$, 4, and 5.

$3lnl'$ configurations have not been observed, indicating that the decays of these configurations do not proceed via K Auger transitions but via L Auger transitions. It is added also that in this work we did not analyze the internal structure of the Auger peaks due to individual states.³³ Details of such an analysis are given by Mack *et al.*,³ Sakaue *et al.*,¹² and Boudjema *et al.*^{35,36} Similar work has been performed by Lin.³⁷

Rather, the main purpose of our work was to determine absolute cross sections for the emission of the K and L Auger electrons and to evaluate the corresponding cross sections for the production of the configurations $2lnl'$ and $3lnl'$. Differential cross sections for electron emission at 0° were obtained by integrating each peak with respect to electron energy (Figs. 2 and 3). In this work we devoted specific effort to the determination of the absolute cross sections. The methods to evaluate absolute cross sections have been described previously.^{8,20} We performed also auxiliary measurements for the $O^{6+} + He$ system and compared the results with our cross section obtained previously.^{20,23}

The measurements of the $O^{6+} + He$ system showed that our previous absolute cross sections must be corrected. We noticed a severe instrumental problem concerning the determination of the gas-cell pressure. After having once calibrated the ratio of the pressures in the gas cell and scattering chamber, we monitored the pressure in the chamber only. This procedure, however, is valid only when the pumping speed of the vacuum pump stays constant. Unfortunately, in some cases, our turbo pump was not operating properly so that its pumping speed changed in an uncontrolled manner. After our first paper⁸ concerning double capture in $O^{6+} + He$ collisions we increased our data by a factor of 4, affecting all absolute cross sections (but leaving cross section ratios essentially unchanged). Now we noticed that this factor of 4 in-

TABLE I. Differential cross sections $d\sigma_I/d\Omega$ ($I=K$ or L) for the production of K and L Auger electrons at 0° following the production of the configurations $2lnl'$ and $3lnl'$, respectively. Also given are the corresponding Auger yields $a_I(n)$. The respective total production cross sections $\sigma_{nlnl'}$ are obtained dividing by the related Auger yield and multiplying by 4π . The indicated errors account only for uncertainties due to statistics and background subtraction.

Configuration	$\frac{d\sigma_I}{d\Omega}(0)$	a_I	$\sigma_{nlnl'}$
	(10^{-18} cm ² /sr)		
$2l3l'$	5.5 ± 0.13	0.66	10.6 ± 0.3
$4l'$	1.05 ± 0.06	0.53	2.5 ± 0.15
$5l'$	0.28 ± 0.04	0.35	1.0 ± 0.16
$6l'$	0.135 ± 0.03	0.29	0.59 ± 0.13
$7l'$	0.055 ± 0.02	0.18	0.37 ± 0.13
$8l'$	0.02 ± 0.02		0.27^a
$\geq 9l'$			0.87^a
$3l3l'$	1.9 ± 0.2	1.00	2.4 ± 0.2
$4l'$	1.05 ± 0.1	1.00	1.32 ± 0.1
$5l'$	0.22 ± 0.06		
$6l'$	0.09 ± 0.04		

^aObtained by extrapolation using the n^{-3} law.

crease was erroneous and that our first results⁸ were correct. Hence all our recent data^{19,21,23} concerning also collision systems other than $O^{6+} + He$ are to be reduced by a factor of 4.

The measured differential cross sections for K and L Auger emission at 0° in the $C^{6+} + He$ system are shown in the first column of Table I. The experimental uncertainties of the absolute cross sections are estimated to be about 40%. The ratio of corresponding cross sections for C^{6+} and O^{6+} impact were measured with an uncertainty of 30%. The errors of the relative cross sections for different Rydberg states given in Table I are primarily

due to counting statistics and uncertainties produced by the subtraction of background. Moreover, as shown in the third column of Table I, from the differential cross sections we derived total cross sections for the emission of K and L Auger electrons by assuming that the electron emission is isotropic. Indications for isotropic electron emission have been found by Boudjema *et al.*³⁵ measuring L Auger spectra at 10° , 90° , and 160° in 60-keV $O^{6+} + He$ collisions. Furthermore, in our previous study²⁰ of electron ejection at 0° and 50° , we have shown that the ratio of the line intensities associated with Coster-Kronig and Auger transitions is constant. It is noted, however, that the information about isotropic electron emission is limited. We expect that the electron angular distributions still need further study.

The derivation of total cross sections has primarily been done to allow for comparison with previous results as shown in Table II. This table will be discussed in more detail below. Here, it is noted only that for the total L Auger electron emission cross section, obtained by summing over the contributions for the configurations $3lnl'$ ($n=3$ to 6), the value of 4.2×10^{-17} cm² is obtained. It agrees within the combined experimental uncertainties with the L Auger emission cross section⁸ of 5.5×10^{-17} cm² for the system $O^{6+} + He$. This confirmed our expectation that the mechanisms for double capture into the equivalent (or near equivalent) electron configurations are similar for the isocharged systems $C^{6+} + He$ and $O^{6+} + He$.

The mechanisms for the production of the nonequivalent electron configuration $2lnl'$ ($n=6$ and 7) in the $C^{6+} + He$ system initially appear to be different from that for $O^{6+} + He$, since the corresponding cross sections differ significantly for the two systems. For instance, the electron production cross section associated with the $2l6l'$ configurations for $C^{6+} + He$ is about a factor of 4 smaller than the corresponding result that we measured for the $O^{6+} + He$ system.⁸ However, this conclusion is premature, since deviation of the Auger yield from 1 has to be taken into account before a comparison is made be-

TABLE II. Cross sections $\sigma_{2lnl'}$ and $\sigma_{3lnl'}$ summed over the quantum numbers nl' produced in the systems $C^{6+} + He$ and $O^{6+} + He$. Also given are the corresponding cross-section fractions. The absolute cross sections from (a) are divided by a factor of 4, see also text. The following references indicate also the electron observation angle. (a) Stolterfoht *et al.* (Ref. 23) (0°). (b) Meyer *et al.* (Ref. 20) (50°). (c) Bordenave-Montesquieu *et al.* (Ref. 28) (10°). (d) Mack and Niehaus (Ref. 9) (50°). (e) Mann and Schulte (Ref. 10) (0°). (f) Chantrenne *et al.* (Ref. 11) (0°). (g) Roncin *et al.* (Ref. 25) (All).

	$C^{6+} + He$	$O^{6+} + He$							
	This work	(a)	(b)	(c)	Other authors	(d)	(e)	(f)	(g)
$\sum_{n=6}^{\infty} \sigma_{2lnl'} (10^{-17} \text{ cm}^2)$	2.2 ± 0.9	2.5		1.2	2.1				2.5
$\sum_{n=3}^{\infty} \sigma_{3lnl'} (10^{-17} \text{ cm}^2)$	4.2 ± 1.7	5.5		14					
$\frac{\sum_{n=6}^{\infty} \sigma_{2lnl'}}{\sum_{n=6}^{\infty} \sigma_{2lnl'} + \sum_{n=3}^{\infty} \sigma_{3lnl'}}$	0.34 ± 0.08	0.31	0.28	0.08	< 0.1	0.40	0.35		

tween the results for the $C^{6+} + He$ and $O^{6+} + He$ systems. The theoretical evaluation of the Auger yield is described in the following section.

III. DATA ANALYSIS AND DISCUSSION

A. Auger yield calculations

In the analysis of the L Auger transitions involving initial states due to the electron configurations $3nl'$ ($n = 3$ and 4) it is assumed that the corresponding L Auger yields $a_L(n)$ are equal to 1 (Table I). The same assumption has previously been made with respect to the Coster-Kronig transitions involving the nonequivalent configurations $2pnl$ in the $O^{6+} + He$ system. The assumption of the unit L Auger and Coster-Kronig yields for O^{4+} has been verified³⁸ using the Hartree-Fock code by Cowan²⁹ in the range of low- n values which is of primary interest here. Thus, in the case of the L Auger transitions for C^{4+} also unit Auger yield was assumed. (Recall also that no experimental evidence was found for K Auger decay of the $3nl'$ configuration).

The high L Auger yield for the equivalent configuration reflects the good spatial overlap between the wave functions of the active electrons involved in the initial and final state. Thus the decay via the competing radiative decay branch is small in the case of the $3nl'$ configurations. However, it is felt that future work is needed to verify the Auger yield for the $3nl'$ configuration. Deviation of the Auger yield from unity may occur for $n \geq 5$. The Auger yield deviations from unity may be responsible for the finding that the cross section for the production of the $3nl'$ electrons in the $C^{6+} + He$ system is about 25% smaller than that in $O^{6+} + He$ (Table II). Nevertheless, no strong Auger yield effects are expected for the $3l3l'$ and $3l4l'$ configurations.

The spatial overlap of the relevant wave functions, however, is significantly poorer when the K shell and higher lying Rydberg states are involved in the Auger transition. Also, since the energy gap involved in the

filling of the K shell is considerably larger, radiative transitions gain in importance so that they may become dominant. Consequently, the Auger yield may deviate noticeably from unity. Then, to evaluate cross sections for the production of the $2lnl'$ configuration from the corresponding cross section for K Auger emission, it is necessary to determine the related Auger yields.

The K Auger yields for the $2lnl'$ configurations ($n = 3$ to 7) were calculated by means of the Hartree-Fock code by Cowan.²⁹ The results for the states associated with the configuration $2l3l'$ are given in Table III. The calculations were performed for two-electron states $|2lnl'\nu J_\nu\rangle$, where J_ν is the total angular momentum and ν labels the states obtained within the framework of the intermediate coupling scheme.³⁹ Configuration mixing with a few significant terms (less than 10) was included in the analysis. It is noted that configuration interaction is expected to be less important for the nonequivalent configurations $2lnl'$ than, e.g., for the equivalent configuration $3l3l'$. As usual, the states are specified by their major configuration and LS component. Transition rates for radiative and nonradiative decay for the state $|2lnl'\nu J_\nu\rangle$ were evaluated to determine the associated K Auger yield $a_K(2lnl'\nu J_\nu)$.

The individual Auger yields were used to obtain the average Auger yield $a_K(n)$ for a given n quantum number by means of the expression

$$a_K(n) = \sum_{l,l',\nu} Q_n(l,l',\nu,J_\nu) a_K(2lnl'\nu J_\nu),$$

where $Q_n(l,l',\nu,J_\nu)$, with the normalization $\sum_{l,l',\nu} Q_n(l,l',\nu,J_\nu) = 1$, is the probability for the production of the state $|2lnl'\nu J_\nu\rangle$ for a given n . We adopted a simple model in which this probability is factorized according to

$$Q_n(l,l',\nu,J_\nu) = q(l)q_n(l')p(J_\nu)s(\nu),$$

where $q(l)$, $q_n(l')$, and $p(J_\nu)$ are the occupation probabilities associated with the quantum numbers l , l' , and J_ν ,

TABLE III. Energies, radiative rates, Auger rates, and Auger yields of states associated with the configuration $2l3l'$. The calculations are performed within the intermediate coupling scheme including configuration interaction. The squared coefficient s for the singlet component are also given. The states are specified by their major configuration and LS component.

State	Energy (eV)	Singlet component	Radiative rate (10^{12} sec^{-1})	Auger rate (10^{12} sec^{-1})	Auger yield
$2s3s \ ^1S_0$	324.564	1.00	0.27	153.6	1.00
$2s3p \ ^1P_1$	323.290	1.00	1.55	0.551	0.26
$2s3d \ ^1D_2$	330.322	1.00	2.31	321.3	0.99
$2p3s \ ^1P_1$	329.156	1.00	1.80	203.9	0.99
$2p3p \ ^1S_0$	332.622	1.00	0.73	4.42	0.86
$2p3p \ ^1P_1$	325.056	0.96	2.85	0.001	0.00
$2p3p \ ^1D_2$	327.516	0.95	2.79	355.7	0.99
$2p3d \ ^1P_1$	331.212	1.00	2.23	36.6	0.94
$2p3d \ ^1D_2$	326.913	0.92	4.11	1.47	0.26
$2p3d \ ^1F_3$	330.659	1.00	6.13	113.2	0.95

respectively, and $s(\nu)$ is the squared coefficient of the singlet component of the intermediate coupling state ν (Table III). The factor $s(\nu)$ takes into account that the two captured electrons are originally in a singlet state and that spin flip can be neglected during the collision. It is found that the states with a dominant triplet component play a minor role in the analysis. The probabilities $q(s)=0.25$ and $q(p)=0.75$ are obtained from the assumption that weighting of the $2s$ and $2p$ subshells is proportional to the number of electrons in each subshell. The probability $p(J_\nu)$ is set to be proportional to $2J_\nu + 1$, which follows from the assumption of a statistical population of the state specified by the total angular momentum J_ν . This statistical model has been used previously in the evaluation of Auger yields.^{40,41} The probability $q_n(l')$ was estimated from recent experimental results²² using also the model by Burgdörfer, Morgenstern, and Niehaus⁴² for extrapolation. For $q_n(l')$ we tested various distributions including the uniform occupation of the quantum numbers l' . We found that the average Auger yield $a_K(n)$ is quite insensitive to the distribution $q_n(l')$, so that we concluded that its choice is uncritical.

The results of the (average) K Auger yield $a_K(n)$ calculations are shown in Table I. It is seen that the K Auger yield deviates increasingly from unity as the quantum number n increases. For instance, the K Auger yield for $n=7$ is only 0.18, which indicates that more than 80% of the decay of the $2l7l'$ configuration proceeds via the radiative decay branch. The Auger yield is reduced by competing K x-ray transitions which are dominant in specific cases. First, within the LS -coupling scheme, K Auger transitions are forbidden because of parity selection rules when $l=L$ in the initial states $(2pnl)L$. In this case Auger transitions may proceed via spin-orbit interaction which, however, is relatively weak (Table III). Second, the Auger yield decreases strongly with increasing l , i.e., the calculations show that the average Auger yield amounts to less than 0.2 for $l=3$ (f state) and is negligible for $l>3$. Because of missing overlap the interaction between the $2p$ electron and the $l\geq 3$ Rydberg electron becomes small so that autoionization loses significance.

The calculated K Auger yields allows the determination of the cross sections $\sigma_{2lnl'}$ for the production of the configuration $2lnl'$ as given in Table I. These cross-section data are also shown in Fig. 4 indicating that they follow the well-known n^{-3} law. It should be emphasized that if radiative decay occurs, both captured electrons remain bound on the ion, and true double capture¹ results. Extrapolating the total cross sections for the productions of the $2lnl'$ configuration by means of the n^{-3} law and assuming a negligible Auger yield for $n\geq 9$, one obtains a value of 7.5×10^{-17} cm² for the true double-capture cross section. This value is not much smaller than the cross section 13×10^{-17} cm² for K and L Auger electron production (Table I).

In Fig. 4 the cross-section results for $C^{6+}+He$ are compared with the corresponding cross sections for the $O^{6+}+He$ system. The latter data are taken from our previous work,²³ taking into account the factor of 4 reduction mentioned before. It is seen that good agreement is obtained between the cross sections for $C^{6+}+He$

and $O^{6+}+He$. This agreement, however, may be accidental as the experimental uncertainty is about 30% for the ratio of the C^{6+} and O^{6+} data. It is recalled that in the $O^{6+}+He$ system only the configurations $2pnl$ can be observed via autoionization. To account also for the $2snl$ configuration one may increase the $O^{6+}+He$ data by the factor $1+q(s)/q(p)=1.33$, assuming again the equal weighting of the $2s$ and $2p$ electrons. In any case, we may conclude that the mechanisms for the production of the nonequivalent configuration $2l6l'$ and $2l7l'$ are closely similar in the two systems as expected from our previous discussion.

In Table II summed cross sections for the production of the configurations $2lnl'$ ($n\geq 6$) and $3lnl'$ ($n\geq 3$) are compared with results from other authors. More information about the data comparison may be found elsewhere.^{25,43} The (summed) cross section for the production of the $2lnl'$ configurations in the $C^{6+}+He$ system was obtained with some extrapolated data using again the n^{-3} law. The present $2lnl'$ production cross section for $O^{6+}+He$ agree well with those by Roncin *et al.*⁶ and Mack and Niehaus.⁹ In the case of the data by Mack and Niehaus⁹ this agreement may be fortuitous since the cor-

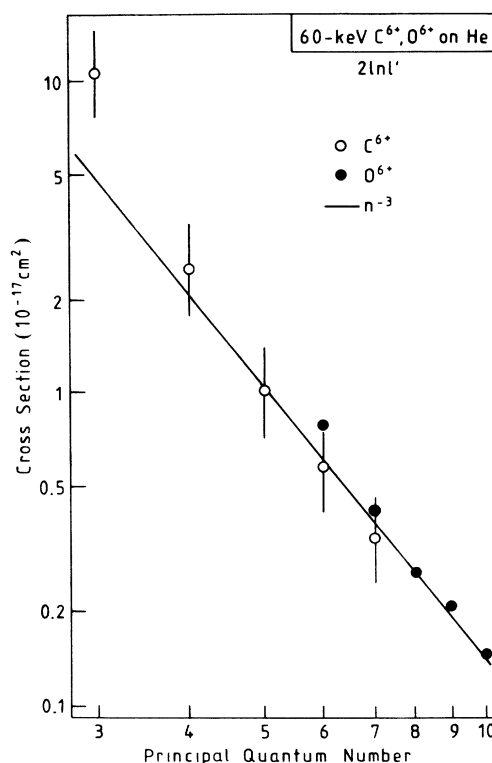


FIG. 4. Cross section for the production of the configuration $2lnl'$ ($n=3$ to 7) in 60-keV $C^{6+}+He$ collisions in comparison with previous cross sections for the 60-keV $O^{6+}+He$ system (Ref. 23). The solid line representing the n^{-3} law is normalized to fit the experimental $C^{6+}+He$. The indicated error bars of 30% are due to the uncertainties in the ratio of the cross sections for C^{6+} and O^{6+} impact; see also text.

responding cross-section fraction (Table II) is smaller than our results by at least a factor of 3. A similar deviation (factor ~ 4) exists between our results and those by Bordenave-Montesquieu and co-workers.^{28,43} On the other hand, our cross-section fraction is in reasonable agreement with the data by Mann and Schulte¹⁰ and Chantrenne *et al.*¹¹ As shown previously,²⁰ the discrepancies are not produced by anisotropic angular distributions of the electrons (see also Table II). It was noted above that the Coster-Kronig transitions associated with the production of the $2pnl$ configuration in $O^{6+} + He$ gives rise to electrons of relatively low energies which are difficult to measure. One of our motivations in using the $C^{6+} + He$ system was the observation of the $2lnl'$ production via K -shell Auger electrons which have rather high energies. The agreement between the cross sections for the systems $C^{6+} + He$ and $O^{6+} + He$ (Table II) gives us confidence that, despite conflicting results from other groups,^{9,28} our previous data for the intensity of the Coster-Kronig lines observed in $O^{6+} + He$ collisions^{8,20} are correct.

B. Discussion of the double-electron-capture processes

We now discuss the electron correlation processes leading to the configurations $2lnl'$ and $3lnl'$ within the framework of the potential-curve diagrams representing the electronic energies of the states relevant for the collision system.^{8,20} Figure 5 shows the potential curves for a limited number of molecular $(C+He)^{6+}$ states which are important for the production of the equivalent $3d^2$ and the

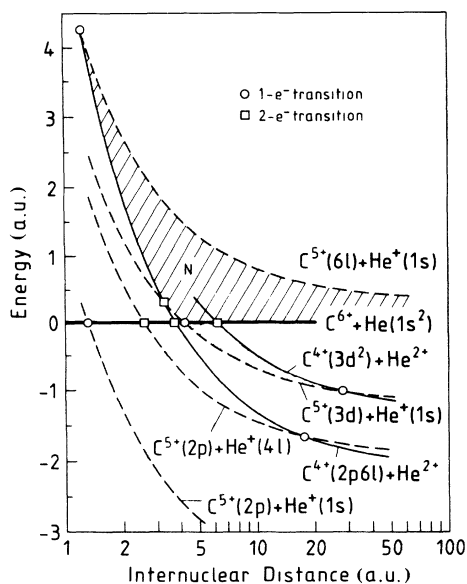


FIG. 5. Potential-curve diagram for the system $(C+He)^{6+}$. The diagram shows a limited number of potential curves relevant for the production of the equivalent configuration $3d^2$ and the nonequivalent configurations $2p6l$. Crossing are indicated where the correlated double capture (CDC) and the correlated transfer excitation (CTE) occurs.

nonequivalent $2l6l'$ electron configurations in C^{6+} . Similarly, Fig. 6 shows potential curves relevant for the production of the nearly equivalent configuration $2p3d$ and the nonequivalent configurations $2pnl$ where $n=4$ and 6. The potential curves are nearly identical to the corresponding curves²³ for $O^{6+} + He$, supporting our earlier suggestion that the characteristic features of the double-capture process are similar for the two systems. Figures 5 and 6 show crossings between potential curves which differ by one spin orbital (circles) and two spin orbitals (squares).⁴⁴ Transitions at the crossing identified by a circle are caused by a one-electron interaction such as radial coupling, whereas transitions at crossings identified by a square require a two-electron interaction such as electron correlation. Second-order effects due to the nuclear-electron interaction causing simultaneous two-electron transitions¹⁶ near a crossing identified by a square are expected to be small for the cases considered in the following.

Each process affecting two electrons may, in principle, be due to a single correlated transition or two independent single-electron transitions. The potential curves followed in these two alternative paths form a "triangle" whose corners consist of two single-electron transitions (circles) and a correlated two-electron transition (square).²³ In Fig. 6 two such triangles are indicated by the hatched areas illustrating that there are striking differences in the alternative paths leading to the production of nonequivalent and (nearly) equivalent electron configuration in $C^{6+} + He$ collisions. It is seen that the triangle N associated with the nonequivalent

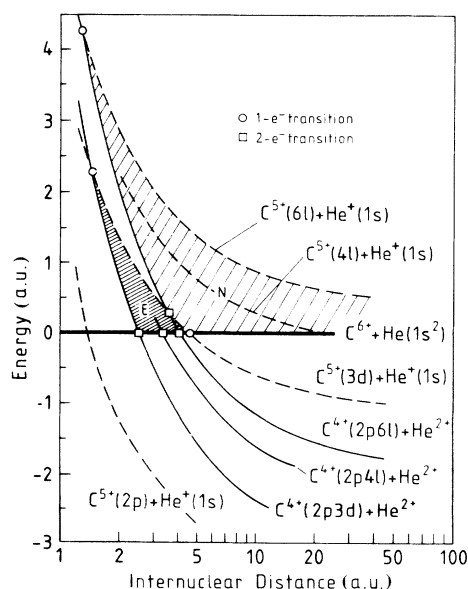


FIG. 6. Potential-curve diagram for the system $(C+He)^{6+}$ as in Fig. 5. The curves are relevant for the production of the nearly equivalent configuration $2p3d$ and the nonequivalent configurations $2pnl$ where $n=4$ and 6.

configuration $2l6l$ is considerably larger than the triangle E attributed to the nearly equivalent configuration $2p3d$.

Before we consider the nonequivalent configuration $2p6l$, the question may be asked of whether electron correlation effects are also important for the production of the equivalent configuration $3l3l'$ or the nearly equivalent configuration $2l3l'$. For the configuration $3l3l'$ this question can be considered as being still open. Barat and collaborators¹⁶ found for the system $O^{8+} + He$ that the nuclear-electron interaction accounts for most of the observed cross sections for the production of the equivalent electron configurations. This conclusion, however, is not necessarily valid for the $O^{6+} + He$ system. The successive single-electron transitions involve a crossing at 4.3 and ~ 30 a.u. (Fig. 5). The transitions at the latter crossing are expected to be rather improbable. Indeed, it should be noted that Roncin *et al.*²⁵ did not observe a production of the configuration $3l3l'$ at an incident energy of 9 keV.

However, at higher energies, such as 60 keV, the state coupling in noncrossing regions, e.g., considered by Demkov⁴⁵ and Nikitin,⁴⁶ gains importance. Close-coupling calculations restricted to the nuclear-electron interaction during the collision performed by Lin⁴⁷ yield a cross section for the production of the $3l3l'$ configuration which is consistent with the present result. On the other hand, the $3l3l'$ configuration may also be produced in a one-step process by means of electron-electron correlation (see the crossing near 7 a.u. in Fig. 5). It is noted that Mack *et al.*³⁴ studied electron-correlation effects in $C^{6+} + H_2$ collisions producing the configuration $3l3l'$. Hence, at present we expect that both correlated and uncorrelated two-electron transitions play a role in the production of the equivalent configuration $3l3l'$. Similar conclusions can be drawn when n exceeds 3 in the configurations $3lnl'$. It is noted that the peak attributed to the configuration $3l4l'$ is rather intense, which may be due to specific promotion mechanisms considered by Roncin *et al.*⁴⁸

For the nearly equivalent configuration $2l3l'$ it is found that its production cross section is relatively large, i.e., it is about a factor of 4 larger than that for the equivalent configuration $3l3l'$ (Table I). Also, Fig. 4 shows that the $2l3l'$ production cross section exceeds even the n^{-3} scaling. Hence it appears that another mechanism enters in the production of the $2l3l'$ configuration. Indeed, Fig. 6 indicates that the $2l3l'$ configuration is most likely produced by a two-step process of single-electron transitions. These transitions take place at crossings near 2 and 4 a.u. which can be shown to lay well within the related reaction window. Hence it is probable that the production of the $2l3l'$ configuration involves uncorrelated electron transitions only. The question of whether a similar conclusion can be drawn for the production of the configuration $2l4l'$ is open.

However, obviously, correlation effects are dominant for production of the nonequivalent configuration $2lnl'$ ($n \geq 5$). The large extent of the triangle N (Fig. 6) illustrates the fact that both one-electron transitions occur well outside the reaction window for single electron capture. In fact, the horizontal curve representing the in-

cident state and the curve labeled asymptotically $C^{5+}(6l) + H(1s)$ do not even cross at large internuclear distances, suggesting that the probability for the corresponding single-electron transitions is small. This feature has been discussed in detail recently,^{23,25} as was the conclusion that uncorrelated single-electron transitions are unimportant for the production of the nonequivalent configuration $2pnl$. Therefore, in the following, we shall focus our attention on the processes involving correlation processes.

Closer inspection of Fig. 5 shows that the production of the $2p6l$ configuration involve a collection of pathways all of which involve correlated two-electron transitions. The correlated-double-capture process⁸ corresponds to the crossing which is seen near the square at 3.8 a.u. formed by the horizontal curve and the curve labeled asymptotically $C^{4+}(2p6l) + He$. The correlated-transfer excitation process²⁶ involves a single-electron transition into the state labeled $C^{5+}(3d) + He^+(1s)$ near 4.3 a.u., followed by a two-electron transition into the final $C^{4+}(2p6l) + He$ state near 3.5 a.u. A further path is seen near 2.5 a.u., where the correlated transfer (target) excitation process occurs which involves the transfer of a He electron to the oxygen $2p$ level and, e.g., the $n=4$ excitation of the other He electron. This two-electron transfer populates the state labeled asymptotically $O^{5+}(2p) + He(4l)$. In a second step the $n=4$ electron is transferred to an nl Rydberg level of oxygen. Thus the $O^{4+}(2p6l) + He^{2+}$ state is populated.

In the following we shall focus our attention on the CDC and CTE processes. As noted already, the role of both processes has been discussed in some detail before.^{23,25,26} Roncin *et al.*²⁵ have shown for relatively low energies of 9 keV that the CTE process is dominant in the $O^{6+} + He$ system. However, at higher energies the system is expected to behave more nonadiabatically, i.e., to follow the incident path rather than to enter the path labeled asymptotically $C^{5+}(3d) + He^+(1s)$. Hence it would be interesting to see whether the conclusion of the dominance of the CTE process holds at higher energies.

Recently, Fritsch⁴⁹ calculated cross sections for the CDC process in 40-keV $C^{6+} + He$ collisions. The impact velocity of 40-keV C^{6+} is nearly equal to that for 60-keV O^{6+} and it is not expected that the velocity difference to 60-keV C^{6+} is essential for the cross sections considered here. The calculations include two-electron coupling matrix elements which are based on the electron-electron interaction. Hence the results shown in Table IV are well suited to model the electron-correlation effects under study here. The calculations are approximated by using a limited number of basis states which were selected to include the main contributors to a given final state. Therefore the basis set varies with the final state. The LS -coupling scheme is used to represent the final state. To study exclusively the CDC process the path associated asymptotically with $C^{6+}(3d) + He^+(1s)$ was not taken into account. However, for the dominant final state 1H this path was added to study also the role of the CTE process (Table IV).

The cross-section data by Fritsch⁴⁹ yield various information. First, it is noted that the calculated distribution

TABLE IV. Theoretical cross sections for the production of the configuration $2p6l$ by double capture in 40-keV $C^{6+} + He$ collisions. The calculations were made accounting for the CDC process only. The data in parenthesis for the 1H state include also the CTE process from Fritsch (Ref. 49).

State	$M=0$ (10^{-17} cm^2)	All M
1S	0.026	0.026
1P	0.09	0.12
1D	0.11	0.29
1F	0.25	0.66
1G	0.21	0.71
1H	0.36 (0.6) ^a	1.2 (2.6) ^a
1J	0.15	0.59
Sum	1.2	3.6

^aIncludes the CTE process.

of the angular momentum is consistent with our previous results²² for the $O^{6+} + He$ system. Second, the theoretical data show that the $M=0$ contribution to the cross section is dominant. (If the M quantum numbers were equally populated the “all- M ” cross section would be $2L+1$ times higher than the $M=0$ result.) This shows that the electron angular distribution is forward peaked. The deviations from the LS -coupling scheme, found in the present Auger yield calculations, complicates the analysis of this anisotropy. Third, it is seen that the theoretical cross sections are significantly larger than the measured results, although it is difficult to perform a detailed comparison because of the uncertainty in the anisotropic angular distribution. Fourth, it is noted that the inclusion of the path associated asymptotically with $C^{6+}(3d) + He^+(1s)$ increases the cross section for the dominant 1H final state by a factor of ~ 2 , indicating that the CDC and CTE processes are of similar importance at the collision energy of 60 keV. This finding in conjunction with the results by Roncin *et al.*⁶ shows that the CDC process gains in importance as the collision energy increases. In any case, the calculations by Fritsch⁴⁹ give conclusive evidence that electron-correlation effects are responsible for the production of the $2p6l$ configuration.

IV. CONCLUSIONS

Cross sections for the emission of K and L Auger electrons were measured following double capture in the system $C^{6+} + He$. Auger yields for the configurations $2nl'$ were derived by means of Hartree-Fock calculations

showing significant deviations from unity. Consequently, the cross sections for true double capture were found to be surprisingly high. With the knowledge of the Auger yield it was possible to determine the $2nl'$ production cross sections. For $n=6$ and 7 these cross sections were found to be in good agreement with corresponding results for the $O^{6+} + He$ system measured previously. In particular, we confirmed our previously measured cross-section fraction for the production of the configuration $2nl'$ ($n \geq 6$) in the $O^{6+} + He$ system for which controversial results exist in literature.

The mechanisms for the creation of the configurations $2nl'$ and $3nl'$ are discussed under the perspective of electron-correlation effects occurring during the collision. The discussion is based on diagrams of approximate potential curves. A relatively large production cross section was found for the configuration $2l3l'$ which is most probably created by uncorrelated single-electron transitions. The question whether the creations of the configurations $2l4l'$, $3l3l'$, and $3l4l'$ are influenced by correlation effects needs further studies. However, the production mechanisms of all configurations involve most likely electron correlation. Hence, using the values in Table I it follows that the cross-section fraction due to the configurations involving electron correlation in relation to all configurations produced by double capture may be as high as 0.5. This value may still increase when the nl Rydberg series are extended into the continuum.²⁴ It would be interesting to see whether this result holds for systems other than $C^{6+} + He$ or $O^{6+} + He$.

Particular attention is devoted to the discussion of the configurations $2nl'$ where $n=6$. It is made conclusively evident that electron correlation is responsible for the creation of this highly nonequivalent configurations. This conclusion is drawn from model calculations of transitions caused by the electron-electron interaction.⁴⁹ Specifically, the calculations show for the collision energy of 60 keV that the correlated-double-capture and the correlated-transfer-excitation processes are of equal importance.

ACKNOWLEDGMENTS

We are indebted to Dr. R. Phaneuf, Dr. M. Barat, and Dr. A. Bordenave-Montesquieu for many clarifying comments. We would like to thank Dr. D. Griffin, Dr. W. Fritsch, and Dr. C. D. Lin for the communication of unpublished results. This work was supported by a NATO Collaboration Research Grant and by the Office of Fusion Energy, U.S. Department of Energy under the Contract No. DE-AC05-84OR21400 with Martin Marietta Energy Systems Inc.

*Present address: Laboratoire de Spectroscopie Atomique, Université de Caen, 14032 Caen, France.

†Present address: Lawrence Livermore National Laboratory, Livermore, CA 94550.

¹D. H. Crandall, R. E. Olson, E. J. Shipsey, and J. C. Browne, *Phys. Rev. Lett.* **36**, 858 (1976).

²T. P. Grozdanov and R. K. Janev, *J. Phys. B* **13**, 3431 (1980).

³M. Kimura and R. E. Olson, *J. Phys. B* **18**, L713 (1984).

⁴S. Tsurubuchi, T. Iwai, Y. Kaneko, M. Kimura, N. Kobayashi, A. Matsumoto, S. Ohtani, K. Okuno, S. Takagi, and H. Tawara, *J. Phys. B* **15**, L733 (1982).

⁵H. Cederquist, L. H. Anderson, A. Bárány, P. Hvelplund, H. Knudsen, E. H. Nielsen, J. O. Pedersen, and J. Sørensen, *J. Phys. B* **18**, 3951 (1985).

- ⁶P. Roncin, M. Barat, H. Laurent, J. Pommier, S. Dousson, and D. Hitz, *J. Phys. B* **17**, L521 (1984).
- ⁷A. Bordenave-Montesquieu, P. Benoit-Cattin, A. Gleizes, A. I. Marakchi, S. Dousson, and D. Hitz, *J. Phys. B* **17**, L127 (1984); **17**, L223 (1984).
- ⁸N. Stolterfoht, C. C. Havener, R. A. Phaneuf, J. K. Swenson, S. M. Shafroth, and F. W. Meyer, *Phys. Rev. Lett.* **57**, 74 (1986).
- ⁹M. Mack and A. Niehaus, *Nucl. Instrum. Methods B* **23**, 116 (1987).
- ¹⁰R. Mann and H. Schulte, *Z. Phys. D* **4**, 343 (1987); R. Mann, *Phys. Rev. A* **35**, 4988 (1987).
- ¹¹S. Chantrenne, M. Prior, R. Bruch, and D. Schneider (unpublished).
- ¹²H. A. Sakaue, K. Ohta, T. Inaba, Y. Kanai, S. Ohtani, K. Wakiya, H. Suzuki, T. Takayanagi, A. Danjo, M. Yoshino, T. Kambara, and Y. Awaya, *Abstracts of Papers, Proceedings of the Sixteenth International Conference on the Physics of Electronic and Atomic Collisions, New York, 1989*, AIP Conf. Proc. No. 205, edited by A. Dalgarno, R. S. Freund, M. S. Lubell, and T. B. Lucatorto (AIP, New York, 1990), p. 570.
- ¹³T. Yamaguchi and A. Ichimura, Ref. 12, p. 573; and private communication.
- ¹⁴A. Bárány *et al.*, *Nucl. Instrum. Methods B* **9**, 397 (1985).
- ¹⁵A. Niehaus, *J. Phys. B* **19**, 2925 (1986).
- ¹⁶M. Barat, M. N. Gaboriaud, L. Guillemot, P. Roncin, and H. Laurent, *J. Phys. B* **20**, 5571 (1987); H. Laurent, M. Barat, M. N. Gaboriaud, L. Guillemot, and P. Roncin, *ibid.* **20**, 6581 (1987); P. Roncin, M. Barat, and H. Laurent, *Europhys. Lett.* **2**, 371 (1986).
- ¹⁷L. H. Andersen, P. Hvelplund, H. Knudsen, S. P. Møller, K. Elsener, K. G. Rensfelt, and E. Uggeerhøj, *Phys. Rev. Lett.* **57**, 2147 (1986).
- ¹⁸N. Stolterfoht, in *Spectroscopy and Collisions of Few-Electron Ions*, edited by M. Ivascu, V. Florescu, and V. Zoran (World Scientific, Singapore, 1989), p. 342.
- ¹⁹F. W. Meyer, C. C. Havener, R. A. Phaneuf, J. K. Swenson, S. M. Shafroth, and N. Stolterfoht, *Nucl. Instrum. Methods B* **24/25**, 106 (1987).
- ²⁰F. W. Meyer, D. C. Griffin, C. C. Havener, N. S. Huq, R. A. Phaneuf, J. K. Swenson, and N. Stolterfoht, in *Invited Papers of the International Conference on the Physics of Electronic and Atomic Collisions, New York, 1989*, AIP Conf. Proc. No. 205, edited by H. B. Gilbody, W. R. Newell, F. H. Read, and A. C. Smith (North-Holland, Amsterdam, 1988), p. 673.
- ²¹N. Stolterfoht, C. C. Havener, R. A. Phaneuf, J. K. Swenson, S. M. Shafroth, and F. W. Meyer, *Nucl. Instrum. Methods B* **27**, 584 (1987).
- ²²F. W. Meyer, D. C. Griffin, C. C. Havener, M. S. Huq, R. A. Phaneuf, J. K. Swenson, and N. Stolterfoht, *Phys. Rev. Lett.* **60**, 1821 (1988).
- ²³N. Stolterfoht, K. Sommer, D. C. Griffin, C. C. Havener, M. S. Huq, R. A. Phaneuf, J. K. Swenson, and F. W. Meyer, *Nucl. Instrum. Methods B* **40/41**, 28 (1989).
- ²⁴J. A. Tanis, D. Schneider, M. Prior, S. Chantrenne, R. Hermann, and R. Hutton, Ref. 12, pp. 596 and 609.
- ²⁵P. Roncin, M. Barat, M. N. Gaboriaud, L. Guillemot, and H. Laurent, *J. Phys. B* **22**, 509 (1989).
- ²⁶H. Winter, M. Mack, R. Hoekstra, A. Niehaus, and F. J. de Heer, *Phys. Rev. Lett.* **58**, 957 (1987).
- ²⁷N. Stolterfoht, C. C. Havener, R. A. Phaneuf, J. K. Swenson, S. M. Shafroth, and F. W. Meyer, *Phys. Rev. Lett.* **58**, 958 (1987).
- ²⁸A. Bordenave-Montesquieu, P. Benoit-Cattin, M. Boudjema, A. Gleizes, S. Dousson, and D. Hitz, in *Abstracts of the Fifteenth International Conference on the Physics of Electronic and Atomic Collisions, Brighton, 1987*, edited by J. Geddes, H. B. Gilbody, A. E. Kingston, and C. J. Latimer (Queen's University, Belfast, 1987), pp. 551 and 552.
- ²⁹R. D. Cowan, *The Theory of Atomic Structure and Spectra* (University of California Press, Berkeley, 1981).
- ³⁰K. Sommer, N. Stolterfoht, J. K. Swenson, C. C. Havener, R. Phaneuf, and F. W. Meyer, Ref. 12, p. 443.
- ³¹A. Itoh, T. Schneider, G. Schiwietz, Z. Roller, H. Platten, G. Nolte, D. Schneider, and N. Stolterfoht, *J. Phys. B* **16**, 3965 (1983); A. Itoh, D. Schnieder, T. Schneider, T. J. M. Zouros, G. Nolte, G. Schiwietz, W. Zeitz, and N. Stolterfoht, *Phys. Rev. A* **31**, 684 (1985).
- ³²N. Stolterfoht, *Phys. Rep.* **146**, 317 (1987).
- ³³Y. K. Ho, *Phys. Rev. A* **23**, 2137 (1981).
- ³⁴M. Mack, J. H. Nijland, P. v. d. Straten, A. Niehaus, and R. Morgenstern, *Phys. Rev. A* **39**, 3846 (1989).
- ³⁵M. Boudjema, P. Benoit-Cattin, A. Bordenave-Montesquieu, A. Gleizes, P. Moretto-Capelle, M. Cornille, J. Dubau, S. Dousson, and D. Hitz, *J. Phys. (Paris) Colloq.* **50**, C1-313 (1989).
- ³⁶M. Boudjema, P. Moretto-Campelle, A. Bordenave-Montesquieu, P. Benoit-Cattin, A. Gleizes, H. Bachau, P. Galan, F. Martin, A. Riera, and M. Yáñez, *J. Phys. B* **22**, L121 (1989).
- ³⁷C. D. Lin, *Phys. Rev. A* **39**, 4355 (1989).
- ³⁸D. C. Griffin (private communication).
- ³⁹K. Sommer, Diplom thesis, Berlin, 1989 (unpublished).
- ⁴⁰C. P. Bhalla, *Phys. Rev. A* **12**, 122 (1975).
- ⁴¹H. Chen and B. Crasemann, *Phys. Rev. A* **12**, 959 (1975).
- ⁴²J. Burgdörfer, R. Morgenstern, and A. Niehaus, *J. Phys. B* **19**, L507 (1987).
- ⁴³A. Bordenave-Montesquieu, M. Boudjema, P. Benoit-Cattin, A. Gleizes, and P. Moretto-Capelle, *J. Phys. (Paris) Colloq.* **50**, C1-305 (1989).
- ⁴⁴J. C. Brenot, D. Dhuicq, J. P. Gauyacq, J. Pommier, V. Sidis, M. Barat, and E. Pollack, *Phys. Rev. A* **11**, 1933 (1975).
- ⁴⁵Y. N. Demkov, *Zh. Eksp. Teor. Fiz.* **45**, 195 (1963) [*Sov. Phys.—JETP* **18**, 138 (1963)].
- ⁴⁶E. E. Nikitin, in *Advances of Quantum Chemistry*, edited by P. O. Löwdin (Academic, New York, 1970), Vol. 5, p. 135.
- ⁴⁷C. D. Lin (private communication).
- ⁴⁸P. Roncin, M. N. Gaboriaud, L. Guillemot, H. Laurant, S. Ohtani, and M. Barat, *J. Phys. B* **23**, 1215 (1990).
- ⁴⁹W. Fritsch (private communication).